



TECHNICAL ARTICLE

Suitability of Pristine Carbon Nanotube Yarn Tool for Material Removal by Electrical Discharges

Sinan Dönmez, Sermet Demir, and Paşa Yayla

Submitted: 7 June 2022 / Revised: 15 November 2022 / Accepted: 11 December 2022

High-intensity electrical discharges are used in the unconventional technique known as electrical discharge machining (EDM) to machine metals of any hardness. Due to their extraordinary conductivity and strength, carbon nanotubes (CNTs) have recently been explored in EDM too. However, material removal with CNT yarn (CNTY) has not been studied thoroughly. This work advocates the use of a pristine CNTY as an EDM tool. The feasibility is examined through characterization and material removal experiments. The measurements show that the CNTY ($< 100 \mu\text{m}$ in diameter) has an electrical conductivity and current carrying capacity of $2.66 \times 10^4 \text{ S/m}$ and $1.76 \times 10^3 \text{ A/cm}^2$, respectively. Steel and aluminum are the workpieces for machining experiments conducted in air and hydrocarbon oil dielectrics, respectively. Significant material removal and extended tool life are obtained in the air dielectric. It is suggested that the oxidation of steel increases material removal in the air while reducing tool life. The effect of tool thickness is also investigated. Thicker ($> 100 \mu\text{m}$) multi-ply tools extend tool life and, therefore, machining time by more than 14 s in the air and nearly 2.5 s in the oil. Other factors that restrict machining include intensified discharges and the shielding effect of the carbide layer formed on the workpiece.

Keywords CNT, carbon nanotube, CNT yarn, EDM, electrical discharge machining, material removal

1. Introduction

Advanced engineering materials have specific properties, such as high strength and stiffness, low thermal expansion, and low weight. However, their high hardness or reinforcing materials make their machining difficult and therefore complicate achieving high precision and surface quality. Thus, non-conventional machining techniques should be employed (Ref 1). Electrical discharge machining (EDM) is a non-conventional method that can machine electrically conductive materials of any hardness without friction or physical contact (Ref 2).

The EDM method involves repetitive short-duration electrical discharges between the tool electrode (cathode) and workpiece (anode). The process is carried out in a dielectric that allows conductive plasma generation between electrodes subjected to high voltage. During these high-intensity discharges, the workpiece quickly melts and evaporates. The procedure is repeated until the desired shape is obtained (Ref 3). Metallic tools with high electrical and thermal conductivities are utilized in this technique (e.g., Copper: 10^7 S/m , 393 W/

mK; Brass: $10^6\text{-}10^7 \text{ S/m}$, 26-233 W/mK; Graphite: 10^4 S/m -25 W/mK (Ref 4, 5)).

Lately, carbon nanotube (CNT) is also studied in EDM. Its excellent electrical and thermal conductivities ($10^4\text{-}10^8 \text{ S/m}$, 20-3500 W/mK (Ref 6-12)) give a strong impression that it may be well suited for such material removal tasks. In this respect, researchers investigated the influence of the powdered or particulate CNTs in EDM by fusing them with the tool electrode material or introducing them into dielectric fluid, also known as powder-mixed EDM (PMEDM).

The PMEDM is an improved EDM technique in which various powders, including silicon, aluminum, chrome, and graphite, are added into the dielectric fluid to obtain a better surface quality, a longer tool life, and a higher material removal rate (MRR) (Ref 13, 14). However, there are concerns about flushing the gap between electrodes due to their high specific gravity and nonuniform dispersion. As a result, the CNTs were mixed with dielectric fluid because of their unique electrical and thermal characteristics, nanoscale size, and strength (Ref 14, 15). For instance, Mohal and Kumar (Ref 14) mixed CNT with dielectric fluid and investigated its effect during the EDM of the Al6061/SiC composite. The primary positive outcomes were higher MRR and surface quality with a widely scattered and more uniform electrical arc. They concluded that the main factor behind those benefits was the improved current transfer due to the high thermal and electrical conductivity of the CNTs in the dielectric. Another study on PMEDM with CNTs revealed that surface quality and machining efficiency improved by 70 and 66%, respectively, compared to conventional EDM. Better results were obtained with CNT powder than with other powders (Si, Al, Graphite). In addition, well-dispersed and homogeneous electrical arcs across the spark gap and, thus, improved discharge performance have been reported as other advantages of CNT use in EDM (Ref 16).

Sinan Dönmez and Paşa Yayla, Department of Mechanical Engineering, Faculty of Engineering, Marmara University, 34840 Istanbul, Turkey; and Sermet Demir, Department of Mechanical Engineering, Faculty of Engineering, Dogus University, 34725 Istanbul, Turkey. Contact e-mails: sinandonmez81@marun.edu.tr, sdemir@dogus.edu.tr, and pasa.yayla@marmara.edu.tr.

The CNTs were also studied in composite EDM tools as a reinforcing material. The aim was to reduce of tool wear and surface roughness. In this regard, Suzuki et al. (Ref 17) investigated the effect of CNT utilization and size on tool wear for pure copper, copper-plated stainless steel, and CNT/Cu-plated EDM tools. Composite electrodes were the least worn tools, with a 50-72% reduction in tool wear ratio. It was also proposed that exposed CNTs on the tool surface prevented further spark erosion of the tool, similar to the effect of turbostratic carbon deposition on the discharge zone.

Besides CNTs, CNT yarn (CNTY), a macroscale thread made of CNT bundles, also has potential for the EDM process. Its wire-like form and small diameter make it suitable for micromachining complex shapes from difficult-to-machine materials, similar to wire-EDM (WEDM). As the EDM method requires electrically conductive tools, several studies show promising results regarding the conductivity of the CNTYs. For example, Choi presented a CNTY-based flexible, lightweight thermo-electric (TE) generator. The results showed enhanced TE properties and indicated that the CNTY had a powerful potential as a TE element. It was emphasized that the CNTYs were used as electrodes to minimize circuit resistance (Ref 18). Furthermore, the CNTYs are even expected to replace metal conductors (Ref 19).

The strength and electrical conductivity of the CNTYs are lower than those of the individual CNTs due to weak inter-tubular interaction among adjacent nanotubes. However, they can carry as much current as graphite, another widely preferred EDM tool material. The electrical conductivity of the graphite is around 10^4 S/m, while the CNTY's conductivity ranges from 10^3 to 10^6 S/m (Ref 7, 20). In addition, the advantages of using graphite tool electrodes are high MRR and low tool wear rates. Therefore, the motivating questions of this study are if the CNTYs are suitable for material removal and whether they provide similar benefits to CNTs and other tool materials in EDM.

As presented above, there are several studies in the literature about EDM with CNT (as an auxiliary material), such as dielectric additive or reinforcement for tools. And for the CNTYs, the research mainly focuses on the conductive properties. However, there are no reports addressing the machining performance of the pristine CNTY tool for EDM on different workpiece materials (Ref 21). Therefore, this study aims to fill this gap by evaluating material removal possibilities. For this purpose, the physical properties of a pristine CNTY were measured through a characterization process and compared with those of another EDM tool material. Then, the feasibility of the material removal with the CNTY was investigated experimentally for different workpieces, dielectrics, and CNTY formations. Finally, obtained results are discussed in detail, considering previous works in the literature.

2. Materials and Methods

This work investigates the feasibility of material removal with a CNTY tool in two phases. In the first stage of the study, the CNTY is characterized in terms of microstructure, mechanical strength, current carrying capacity, and thermal properties. Then, the results are evaluated to determine whether the CNTY possesses the physical qualities required by the EDM process. In the second stage, the machining capability of the CNTY is

investigated through preliminary material removal experiments performed in air and hydrocarbon oil dielectrics separately.

2.1 Materials

The electrical resistance of a tool electrode is significant in EDM because high resistivities result in low metal removal rates (Ref 5, 22). As previously stated, the CNTY's resistivity is comparable to that of graphite, a popular tool material in EDM, due to benefits such as higher MRR and lower tool wear. From the point of view, the CNTs can be assumed as tubular graphite layers (Ref 23). Besides these similarities, the CNTs have specific advantages in EDM, such as higher surface quality and machining efficiency (Ref 16). In addition, the thin and wire-like structure of the CNTY could enable it to cut complex micro-geometries out of hard materials, as in the case of μ EDM. Therefore, CNTY was chosen as a tool material to investigate whether it could be used with similar advantages as CNTs and graphite.

On the other hand, various elements, such as changes in the diameter of CNT filaments, impurities, voids, doping material, and twist angle, can significantly affect the overall physical properties of the CNTYs (Ref 24, 25). Therefore, a pristine CNTY was preferred to reduce such external factors. The same approach has been adopted for the brass wire selection in the characterization section. Also, carbon steel and aluminum were chosen as workpiece materials because these are the most favored conductive materials in engineering applications. Air is used as a dielectric medium since it has certain benefits, such as lower tool wear and higher material removal rates (Ref 26). In addition, conventional EDM oil is also utilized, as it can limit and eliminate oxidation, which can accelerate the decomposi-

Table 1 Test materials and specifications

Tool material	CNTY (Nanoworld Lab of University of Cincinnati—USA)
Tool thickness, μm	Single-ply ($\sim 100 \mu\text{m}$), multi-ply (various)
Ply quantity of tool, pcs	Single-ply (1), multi-ply (2, 3, 5, 10)
CNT types of the CNTY	Double and triple-walled CNTs
Reference material for characterization	Brass (OB-PZN series—OKI Electric Cable Co., Ltd.—JAPAN)
Reference material thickness, μm	$\sim 100 \mu\text{m}$
Workpiece materials	Carbon steel, aluminum
Workpiece thickness, mm	$\varnothing 1.3$ mm (steel), $\varnothing 4$ mm (aluminum)
Dielectrics	Air, hydrocarbon oil (CAS no: 64771-72-8, C5-20)
EDM machines	OscarMax S550 NC

Table 2 Test devices

Microscope	Jeol JCM-6000 Plus SEM (w EDX)
Microbalance	Mettler Toledo MX5
Tensile tester	Instron 4411
Multimeter	Keithley 2450 SourceMeter, Agilent 34405A
Power supply	Agilent E3642A
IR Camera	FLIR

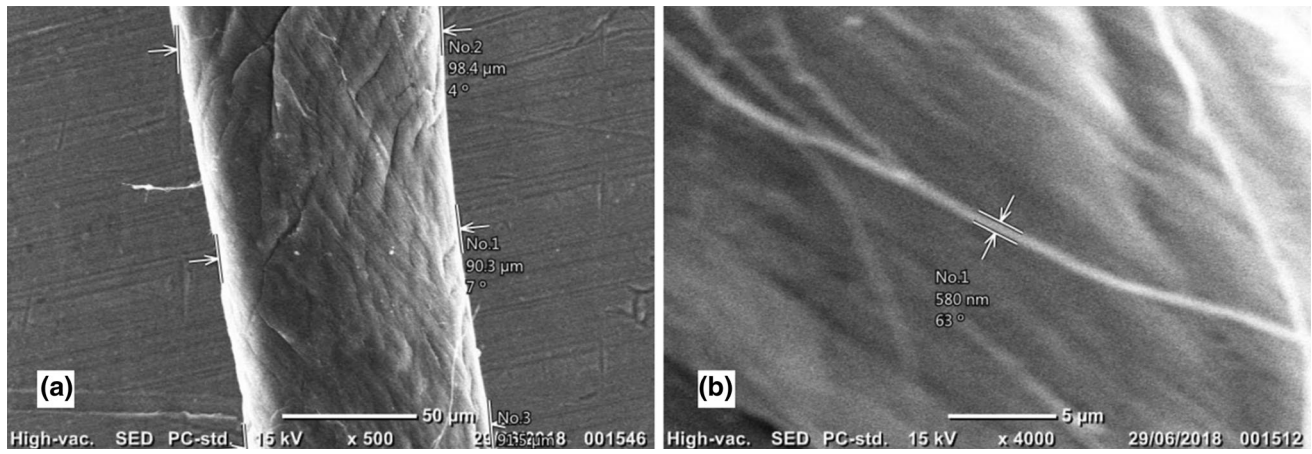


Fig. 1 Thickness measurements (a) Diameter of the CNTY at different locations (top 98.4 μm , middle 90.3 μm , bottom 91.5 μm), (b) Thickness of a flyaway fiber (bundle-580 nm) on the CNTY

tion of the CNTY. Preferred materials and test devices are given in Table 1 and 2.

2.2 Characterization

Several measurements were performed to reveal the CNTY's features. Firstly, scanning electron microscopy (SEM) was utilized to obtain the apparent thickness and microscale properties. Chemical composition was also characterized by energy-dispersive x-ray spectroscopy (EDS). After that, the tensile strength was measured. The maximum electrical current carrying capacity was also determined, along with electrical resistance. In addition, all the results were compared to a commercial wire-EDM electrode for a more consistent interpretation.

2.2.1 Microscopic Properties and Chemical Composition. The cross-sectional thickness measurements of the CNTY were made at ten different locations. The gold plating was not applied as the CNTY has sufficient conductivity. General appearance and thickness measurements can be seen in Fig. 1(a). Individual fiber or bundle thickness was also measured (Fig. 1b). The results are presented in Table 3. Energy-dispersive x-ray spectroscopy (EDS) revealed that most of the yarn was composed of carbon. In addition, the twist angle (α) was measured as approximately 28°, Fig. 2.

2.2.2 Linear density. The cross section of a CNTY is neither a basic shape (for example, a perfect circle) nor is it longitudinally constant (Ref 27), resulting in different physical property measurements on the same yarn. As a result, it is not straightforward to determine the cross section and, thus, the physical properties (Ref 24, 28). Therefore, material-specific properties, such as linear density, were preferred over general non-specific properties (Ref 29, 30). The linear density was calculated as $\text{Tex} = 4.133$ (mg/m). This property was also utilized for strength calculations.

2.2.3 Mechanical Properties. The tool should be stable during the EDM process. Otherwise, the machining precision cannot be maintained. Tensioning the tool electrode is a common practice in WEDM. It reduces undesired movements and improves machining stability (Ref 31). However, the mechanical strength of a tool must be known to apply the tension safely. For this reason, a tensile tester was utilized at a strain rate of 0.1 min^{-1} . The initial length of the CNTY

Table 3 Measured thickness values of the CNTY

	Min	Max	Average	Std. Dev., σ
Overall thickness, μm	90.3	111	96.95	6.5
Flyaway fiber (bundle) thickness, nm	44.6	1480	460.36	285.54

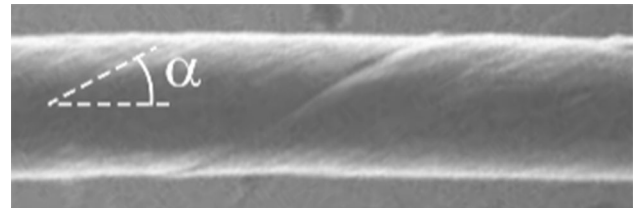


Fig. 2 Twist angle of the CNTY

specimens was 50 mm. The obtained load-extension behavior of the yarn is shown in Fig. 3. The numerical data for the tensile test results are presented in Table 4.

CNTYs have high porosity, dramatically affecting the yarn strength. Therefore, even a small amount of load can easily change the diameter of the CNTY specimen as the spaces among the CNT bundles disappear with a tensile load. This effect was observed as scatter values in the initial part of the test. Therefore, yarn-specific stress was preferred (N/tex). By using the tex value (4.133 mg/m) and average tensile load (1.08 N), the specific strength of the CNTY was calculated as 0.26237 N/tex. In addition to the results presented above, the average strength of the CNTY was also determined, assuming the material was continuous and its cross section was circular. This was preferred to be able to make a rough comparison. As a result, the average tensile load at break was calculated as 1.0845 N. The cross-sectional diameter was accepted as 96.95 μm , and the corresponding tensile strength was calculated as 146.91 MPa.

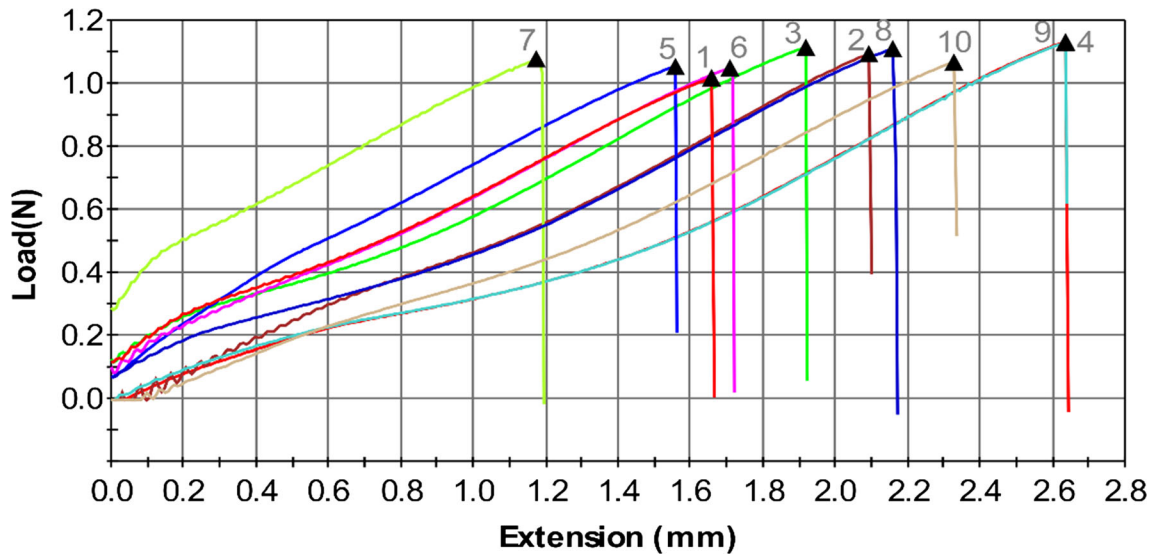


Fig. 3 Load-extension behavior of CNTY specimens

Table 4 General tensile test results

	Min	Max	Average	Std. Dev., σ
Tensile load (N)	1.08	1.13	1.08	0.038
Strain (%)	2.34	5.26	3.97	0.95

2.2.4 4 Electrical Properties. The resistivity of the tool electrode is critical because it dramatically affects EDM performance (Ref 32). Therefore, four-probe resistance measurements were performed on multiple specimens. After that, electrical resistivity ρ ($\Omega\cdot\text{m}$) and conductivity σ (S/m) were calculated by using Eq 2.1 and 2.2, respectively:

$$\rho = R \frac{A}{l} \quad (\text{Eq 2.1})$$

$$\sigma = \frac{1}{\rho} = \frac{l}{RA} \quad (\text{Eq 2.2})$$

where R is the measured electrical resistance (Ω), l is the specified length (in this case, $l = 0.05$ m), and A is the yarn's cross-sectional area (m^2). The measured average resistance (R) of the CNTY was 254.38Ω . The average resistivity was calculated as $3.756 \times 10^{-5} \Omega\cdot\text{m}$, and the corresponding electrical conductivity was calculated as 2.66257×10^4 S/m. Besides conductivity, the maximum current that the conductor can withstand is also important. Thus, the current carrying capacity (ampacity) of the CNTY was measured, Fig. 4(a). A simplified test setup can be seen in Fig. 4(b). During the test, the electrical load was gradually increased. At each step, the voltage was kept constant until the temperature was stabilized. When a test specimen reaches a critical temperature, it begins to degrade, and its resistance increases until it breaks. This temperature was also recorded, Fig. 4(c). The minimum current at rupture was recorded as 0.1259 A at 25.336 V, while the maximum was 0.1471 A at 24.41 V. The rupture temperature due to extreme heat varied between 499.15 K (226 °C) and 536.15 K (263 °C). Moreover, the CNTY is a novel material, not a commercial EDM tool. For this reason, a brass wire-EDM

electrode was used as a reference to evaluate the measurement results of the yarn consistently. The brass wire has undergone the same characterization process as seen in the section below.

2.2.5 Characterization Results. The physical properties of the CNTY and the brass wire obtained through the characterization process are given in Table 5. The electrical resistivity of the CNTY corresponds to a conductivity of 2.66×10^4 S/m. A comparison with other EDM tool materials is shown in Fig. 5. The CNTY has a conductivity slightly higher than graphite's (1.67×10^4 S/m) and lower than the conductivity levels of brass, molybdenum, tungsten, and copper, which vary between 10^6 and 10^7 S/m (Ref 4, 5). In addition, during the ampacity test, the maximum temperatures at the break for CNTY and brass wire were recorded as 513.15 and 533.15 K, respectively. Consequently, the CNTY seems suitable for material removal regarding electrical conductivity and thermal resistance. On the other hand, experimental work is necessary to confirm its applicability. In the next section, material removal tests are presented.

3. Experimental Procedure

Preliminary material removal experiments were performed on carbon steel and aluminum workpieces in air and hydrocarbon oil dielectrics, respectively. The electrical polarity was negative for the CNTY and positive for the workpiece. The CNTY was used in single-ply ($\sim 97 \mu\text{m}$) and in thicker multi-ply formations to observe the effect of yarn thickness on machining. The multi-ply structure was obtained by winding a single CNTY on two parallel pins several times, then twisting it to reduce newly created voids and increase stiffness. The multi-ply formation also increased the number of adjacent fibers in a unit volume and improved heat dissipation from the spark zone. In this way, the machining period was aimed to be extended.

A steel wire of 1.3 mm in diameter was used as workpiece material. The EDS detected Fe, C, and Al as the primary alloying elements. Average mass fractions were 94.79, 4.07, and 1.15, respectively. Moreover, single-ply CNTY was relatively thin ($97 \mu\text{m}$) compared to common wire-EDM

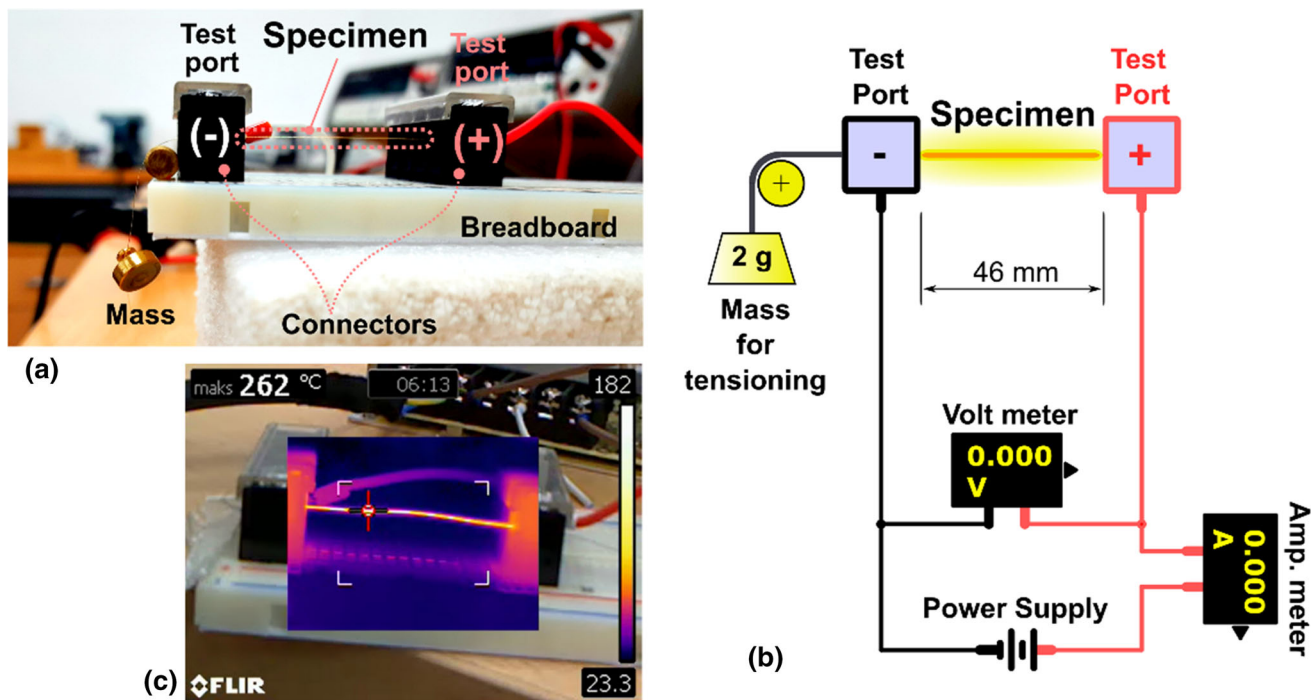


Fig. 4 (a) Ampacity test apparatus, (b) Simplified schematic of the test setup, (c) One of the infrared temperature measurements

Table 5 Measured properties of CNTY and brass wire

Measured Physical Properties (Average)	CNTY	Brass wire-EDM tool
Diameter, \varnothing	96.95 $\mu\text{m}^{(a)}$	101.68 μm
Tensile strength, σ	146.91 MPa ^(b) (0.26 N/tex)	1268 MPa
Electrical resistivity, ρ	$3.756 \times 10^{-5} \Omega\cdot\text{m}$	$8.168 \times 10^{-8} \Omega\cdot\text{m}$
Ampere, voltage, and temperature at rupture	0.13 A, 24.27 V, $\sim 513.15 \text{ K}$	1.85 A, 3.90 V, $\sim 533.15 \text{ K}$
Ampacity, A/cm^2	$1.76 \times 10^3 \text{ A}/\text{cm}^2$	$2.2782 \times 10^4 \text{ A}/\text{cm}^2$

(a): The CNTY's cross section might not be perfectly circular, (b): The strength value in Pascal is calculated for rough comparisons by assuming the cross section is circular and continuous.

electrodes (generally, 0.15-0.25 mm wires are preferred (Ref 31)). In addition, CNTYs do not have the thermal and mechanical strength of individual CNTs, so they are vulnerable to extreme heat and pressure increases where the electrical discharge takes place. Therefore, the EDM machine was set to a low ampere level (1 A).

In the first material removal experiment, the CNTY was placed between the brass clamping plates of an electrode holder. The required tension was applied manually and stabilized by tightening the screws (Fig. 6). At the beginning of the test, the CNTY was positioned close to the workpiece (Fig. 7a). Then, the machining was started in an air dielectric. An electrical spark was observed when the gap between the tool and the workpiece decreased to a critical level (Fig. 7b). This is noteworthy as the electrical arc generation between the tool and workpiece is the first and most essential step of the EDM. During machining, the machine periodically stopped the pulsed current application (spark operation) by moving the CNTY up a few millimeters in the z-axis to facilitate cooling. Finally, it returned to the original point where the spark occurred and continued the process. These spark-up-down (SUD) cycles were repeated until the rupture of the yarn.

In experiments with thick multi-ply yarns, the spark process varied between about 208 (milliseconds) and 530 ms, with an average of 370 ms. A peak current of 1 A was applied during each spark period. On-time was 25 μs , off-time was 90 μs , and the corresponding duty cycle of the pulsed current was calculated as 21.74%. The CNTY endured a spark period of approximately 14.43 s (seconds). This period corresponds to 39 SUD cycles (pulse-on and pulse-off times are included in this sum, but intermittent cooling periods are excluded). The machined area on the workpiece is shown in Fig. 8a. The extent of the material removal can be seen in Fig. 8(b) and (c)

For the second experiment, an improved holder with tensioning was manufactured. A simplified diagram can be seen in Fig. 9a. The CNTY was attached to the holder. A spring applied the required axial force on the yarn, and the tensioning grip was then fixed to stabilize it. The liquid dielectric was also utilized to remove excess heat and re-solidified particles with this particular setup. Another benefit of hydrocarbon dielectric was less oxidation possibility during machining. A cylindrical aluminum alloy was used as the workpiece. Similar to the first experiment, single and multi-ply CNTY tools were used. The thicknesses of multi-ply yarns are not specified in Table 6 as

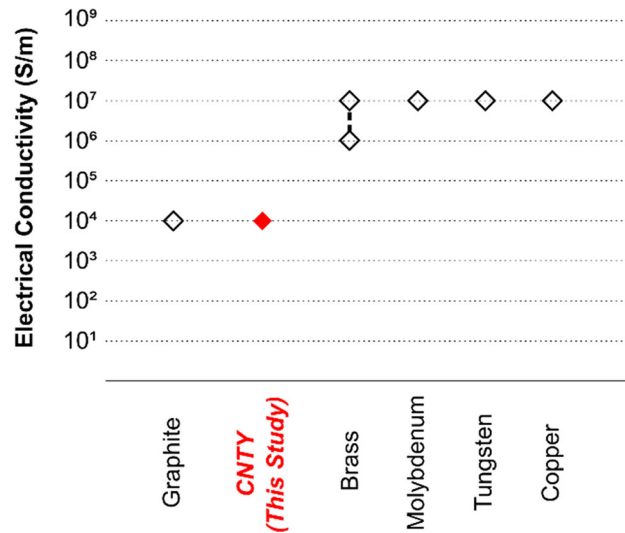


Fig. 5 Electrical conductivity comparison of the CNTY and other metallic materials

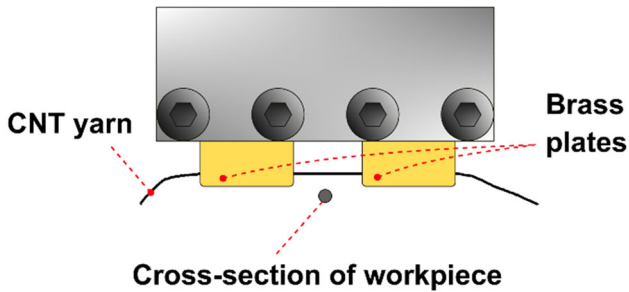


Fig. 6 Schematic for the first material removal setup

they do not have a regular cross section. However, the estimated cross sections are presented in Fig. 10 for illustrative purposes. The tests were carried out with nine different parameters and five yarn formations, Table 6. The experiment was started with a single-ply CNTY tool and a peak current of 0.5 A. Then, yarn formations and peak currents were modified. Higher peak currents were also tested to create a larger discharge gap between the tool electrode and the workpiece. Thus, the dielectric could dissipate excess heat more efficiently, and less heat would be transferred to the tool.

With multi-ply yarns, the spark time was longer than the time obtained with single-ply yarn, as in the first trial. This time, a maximum of three SUD cycles were performed. The total successful spark period was 2472 ms. When the machining zone of the workpiece was examined, carbon deposition on the surface was evident (Fig. 9b). Once this carbon soot was cleaned, a small heat-affected zone was revealed (Fig. 9c), yet the material removal was negligible. Consequently, increasing the thickness of the CNTY by adding more plies improved the EDM spark period in the first and second material removal experiments. The results are summarized in Table 7. The following section discusses possible reasons for the results, encountered problems, and necessary improvements.

4. Discussion

This study investigated the suitability of the pristine CNTY tool for material removal with electrical discharges and verified it experimentally. The results indicated that the thickness of the tool was critical in terms of tool life and, thus, machining time. In addition, the oxidation improved material removal from steel, but it also limited tool life. Intensified discharges and carbide layer formation were other limiting factors. Details are discussed in two subsections below.

4.1 Evaluation of the Characterization Results

The mechanical properties of the CNTY match previous research results (Table 8). The electrical conductivity of the CNTY was found as 2.66×10^4 S/m, which is consistent with the range of 1.5×10^4 S/m- 4.1×10^4 S/m reported previously (Ref 33). In addition, a comparison with other EDM tool materials (Fig. 5) suggests that the CNTY has sufficient conductivity for EDM. Besides, the CNTY and the brass EDM wire had similar thermal strengths under electrical load during the ampacity test, Table 5. Consequently, these electrical and thermal property similarities are considered as indicators of the CNTY's suitability for EDM.

4.2 Evaluation of the Material Removal Experiments

At the first test performed in air, the maximum machining depth and spark time achieved on the steel workpiece were around 0.2 mm (Fig. 8c) and roughly 14.5 s, respectively. The spark time was found to be directly proportional to the tool thickness. In addition, the oxidation of the CNTY is proposed as the main factor limiting tool life. Then, the second test was conducted in an oxygen-free hydrocarbon oil. Contrary to expectations, less tool life (~ 2.5 s) was obtained. A heat-affected zone was observed on the aluminum workpiece without any noticeable material removal (Fig. 9c). This is attributed to a smaller working gap due to the higher dielectric strength of the oil compared to air and, thus, more intensified discharges. The key factors and their effects are summarized in Table 9 and discussed in the following subsections.

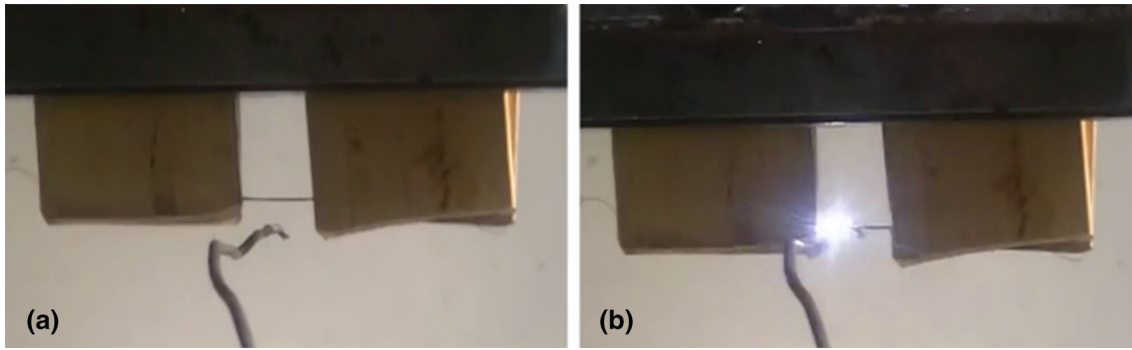


Fig. 7 (a) Tool electrode (the CNTY) is above the metal wire, (b) Emerging electrical arc during machining

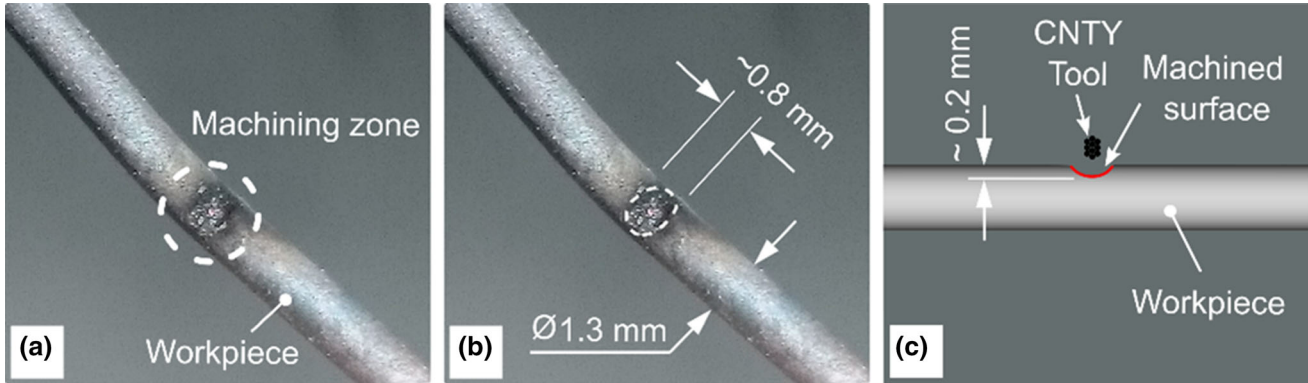


Fig. 8 Machined zone on the steel wire (a), the width of the crater (0.8 mm) is larger than the tool's thickness due to spark gap (b), a cross-sectional schematic of the machining zone (c)

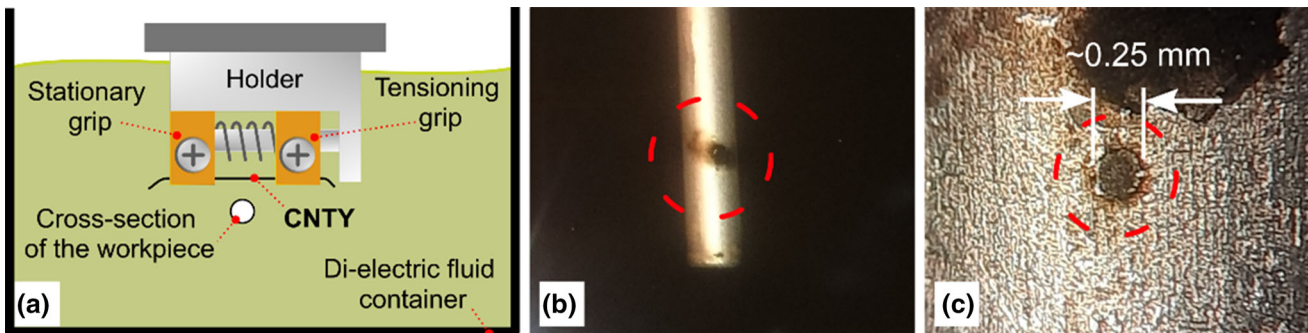


Fig. 9 Setup for the second material removal experiment (a). Material removal on the aluminum workpiece was negligible due to the thermal shielding effect of the carbon-deposited surface (blackened area) (b). When this carbon soot was cleaned, a circular heat-affected zone was exposed (c)

4.2.1 Ply Quantity (Tool Thickness). The experiments showed that the tool thickness significantly affects tool life. Thicker multi-ply yarns increased the tool life, and thus the spark time, by more than 14 s in air and nearly 2.5 s in the oil dielectric. Other process modifications were not as effective as increasing the CNTY thickness. This is because the thinner electrodes are affected by more discharges per unit area. As a result, more heat is concentrated in a smaller zone (Ref 34), causing faster destruction of the EDM tool.

4.2.2 Oxidation. At the first machining test (applied in air dielectric), higher material removal and longer tool life were observed due to the extra heat from the oxidation of the steel.

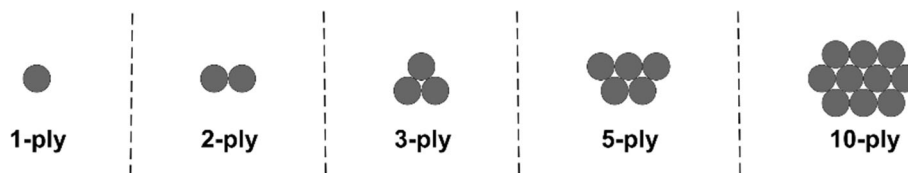
Electrical discharges during machining generate heat, increasing the oxidation rate of the workpiece (Ref 35). Since oxidation is generally exothermic, it generates additional heat in the spark zone (Ref 26). Hence, discharge intensity increases (Ref 35), and more material removal per pulse is achieved (Ref 36). The MRR is also directly proportional to the oxygen concentration in the air. Furthermore, very low tool wear is another advantage of EDM in an oxygen-containing gas (Ref 37).

Oxidation adversely affects the integrity of the CNT. Oxygen breaks down CNTs and creates CO and CO₂ when the temperature exceeds ~ 600 K. This phenomenon results in the opening of closed CNTs and thinning (layer-by-layer

Table 6 Parameters of the second material removal experiment

Test code	CNTY ply number and thickness, μm	Workpiece	Voltage, V	Ampere, A
S1P1	1 ply ($\sim 97 \mu\text{m}$)	Al	50	0.5
S2P1	1 ply ($\sim 97 \mu\text{m}$)		45	3
S3P1	1 ply ($\sim 97 \mu\text{m}$)		40	6
S4P2	2 plies*		50	0.5
S5P2	2 plies*		45	3
S6P3	3 plies*		45	3
S7P5	5 plies*		50	0.5
S8P10	10 plies*		30	6
S9P10	10 plies*		50	0.5

*Multi-ply CNTYs that do not have circular cross sections. Therefore, the proper diameter or thickness measurements could not be performed for those threads.

**Fig. 10** Estimated cross sections of yarns having different ply numbers**Table 7 Machining parameters and results of the material removal experiments**

Test	Dielectric	CNTY formation	Peak ampere, A	SUD cycles	Spark time, s
1st	Air	Single-ply	1
		Multi-ply	1	39	14.43*
2nd	EDM oil	Single-ply	0.5
		Multi-ply	0.5	3	2.47*

* The spark times show the maximum value obtained during the test. They were calculated by adding separate spark periods from the best test run. Intermittent cooling times are excluded.

destruction) of MWNTs, as demonstrated by Ajayan and Kunieda (Ref 38, 39). The degradation temperature could be as low as 623 K (350 °C) (Ref 40, 41). Therefore, oxygen in the air dielectric probably accelerated the breakdown of the CNTY during our experiments.

The oxidation has a significant influence on the current carrying capacity (or ampacity) as well. In this study, the ampacity of the CNTY was measured as $1.76 \times 10^3 \text{ A/cm}^2$, which is lower than a recent measurement performed in a vacuum ($\sim 1.78 \times 10^4 \text{ A/cm}^2$) (Ref 42). This is common for CNT-based conductors subjected to current-induced Joule heating. The CNT-based fibers generally fail at lower temperatures in the air due to oxidation compared to tests performed in an inert atmosphere or vacuum (Ref 43, 44). As a result, the destructive effect of oxygen limited the tool life and machining time in the first experiment.

In the second material removal experiment, an oxygen-free hydrocarbon oil was used instead of air to eliminate the effect of oxygen and improve cooling. However, less tool life and negligible material removal were obtained, suggesting that the mechanism behind this result must be different from oxidation. The following sections focus on these factors.

4.2.3 Intensified Discharges. The hydrocarbon dielectric oils have higher dielectric strengths than air, Table 10. Therefore, higher discharge energy or a smaller working (or discharge) gap is required to initiate the spark (Ref 45, 46). Also, lower oil viscosity limits the plasma expansion, concentrating discharges in a smaller zone (Ref 46). As a result, intensified discharges increase the disintegration of the CNTY. When coupled with the weak attraction forces among CNT bundles (Ref 47, 48), this phenomenon may have accelerated the failure of the CNTY tool. Additionally, flushing loses efficiency as working distance decreases, leading to instability, short circuits, and tool wear (Ref 45). Consequently, reduced tool life due to more powerful discharges, and carbide layer formation on the aluminum workpiece are proposed as the main reasons for negligible material removal at the second machining test.

4.2.4 Carbide Layer Formation on the Workpiece. When hydrocarbon oils are used as dielectrics, excessive heat from electrical discharges chemically breaks down the oil, producing carbon particles. Because the energy dissipation into the anode is more significant during these electrical discharges, more particles precipitate on the workpiece and form a heat-resistant carbide layer (Ref 49). As a result, the

Table 8 Mechanical property comparison of the CNTY and prior data

Test	This study	Deng et al. (Ref 55)	Yang et al. (Ref 56)
Tensile Strength, MPa	146.91 ^(c)	82–490	124.4
Strain, %	3.97	3–12	0.153

(c): Average tensile strength has been calculated by assuming the cross section is circular, and the material is continuous.

Table 9 Key factors and their influence on tool life and material removal

Test	Factors	Impact on tool life	Impact on material removal	
1st	Tool: CNTY, Workpiece: Steel, Dielectric: Air	Oxidation	(-)	(+)
		Increasing tool thickness	(+)	(+*)
2nd	Tool: CNTY, Workpiece: Aluminum, Dielectric: Hydrocarbon oil	Intensified discharges	(-)	(-*)
		Increasing ply quantity	(+)	(+*)
		Carbide layer on the workpiece	(-*)	(-)

(+): Direct positive impact, (-): Direct negative impact, (+*): Indirect positive impact, (-*): Indirect negative impact.

Table 10 Specific properties of common dielectric media used in EDM (Ref 57)

	De-ionized water	Kerosene/hydrocarbon oils	Air
Dielectric strength, MV/m	13	14-22	3
Dynamic viscosity, g/m.s	0.92	1.64	0.019
Thermal conductivity, W/m.K	0.606	0.149	0.026
Heat capacity, J/g.K	4.19	2.16	1.04

EDM becomes unstable, and consequently, the MRR drops (Ref 50). In conclusion, this mechanism might have been the reason for the negligible material removal from the aluminum workpiece. The blackened surface on the test specimen supports the carbon deposition concept (Fig. 9b).

4.3 Future Scope

Certain improvements for the CNTYs can be studied in the future. For example, the overall strength of the CNTYs can be improved with densification and increasing inter-tubular interactions by creating covalent bonds among individual CNTs or by cross-linking. These cross-linking techniques could be chemical treatments, irradiation, and incandescent tension annealing (ITAP) (Ref 51-53). The ITAP technique also increases the oxidative strength of the nanotubes (Ref 53). In addition, EDM can be performed in a vacuum or an inert atmosphere to reduce the effect of oxygen. For instance, Takahata et al. attempted the machining of CNT forests by μ EDM in air or oxygen dielectric. They indicated that proper CNT removal might not be possible without oxygen (for example, in 100% nitrogen gas dielectrics) (Ref 54).

5. Conclusion

This study investigated the suitability of the CNTY for material removal from metals using electrical discharges. The conclusions are summarized below.

1. Initial tests have shown that material removal with a pristine CNTY tool is possible.
2. Tool thickness is critical for spark time. Longer tool life and machining time were achieved with thicker ($> 100 \mu\text{m}$) multi-ply tools. The spark time in the air dielectric increased to 14.5 s until tool failure. This period was 2.5 s for the tests performed in hydrocarbon oil dielectric.
3. The oxidation determined the MRR and tool life during machining. The use of air dielectric improved material removal from steel because of the additional heat generated by exothermic oxidation reaction. However, it also reduced the CNTY's material strength and tool life by disintegrating the CNTY as CO and CO₂.
4. More focused and intensified discharges occurred in hydrocarbon oil dielectric due to a smaller discharge gap as a result of the higher dielectric strength and viscosity of the medium. This situation reduced tool life more than in the case of air dielectric.
5. The precipitated carbon particles, produced by the breakdown of oil, formed a heat-resistant carbide layer on the workpiece and made material removal difficult. As a result, more material removal was obtained in the air medium than in the liquid dielectric.

It is predicted that the CNTY could be a competitive tool alternative for micromachining hard engineering materials when its thermal and mechanical strengths are further improved. Moreover, the behavior of a pristine CNTY during

EDM has not yet been explored in the literature. This study investigated the material removal capacity of the CNTY to close this research gap. Because of that, further tasks such as optimization of MRR or surface roughness are not included in this research.

Acknowledgments

This study was funded by the Scientific Research Projects Coordination Unit of Marmara University (BAPKO) in Istanbul, Turkey [project number FEN-C-DRP-100616-0282]. We would like to thank the academics at Marmara and Dogus Universities for contributing to this research.

Author Contributions

SD contributed to conceptualization, methodology, investigation, writing—original draft, visualization, resources. SD contributed to conceptualization, methodology, investigation, writing—original draft, resources. PY contributed to writing—review and editing, supervision, project administration, resources.

Funding

This study was funded by the Scientific Research Projects Coordination Unit of Marmara University (BAPKO) in Istanbul, Turkey [project number FEN-C-DRP-100616–0282].

Conflict of interest

The authors have no relevant financial or non-financial interests to disclose.

References

1. R.K. Garg, K.K. Singh, A. Sachdeva, V.S. Sharma, K. Ojha, and S. Singh, Review of Research Work in Sinking EDM and WEDM on Metal Matrix Composite Materials, *Int. J. Adv. Manuf. Technol.*, 2010, **50**(5–8), p 611–624. <https://doi.org/10.1007/s00170-010-2534-5>
2. N. Mohd Abbas, D.G. Solomon, and M. Fuad Bahari, A Review on Current Research Trends in Electrical Discharge Machining (EDM), *Int. J. Mach. Tools Manuf.*, 2007, **47**(7–8), p 1214–1228. <https://doi.org/10.1016/j.ijmactools.2006.08.026>
3. M.P. Jahan, M. Rahman, and Y.S. Wong, A Review on the Conventional and Micro-Electrodischarge Machining of Tungsten Carbide, *Int. J. Mach. Tools Manuf.*, 2011, **51**(12), p 837–858. <https://doi.org/10.1016/j.ijmactools.2011.08.016>
4. S. Kalpakjian and S.R. Schmid (2013) *Manufacturing Engineering and Technology*, H. Stark and C. Romeo, Eds., 7th ed., Pearson Education Limited
5. T. Czelusniak, C.F. Higa, R.D. Torres, C.A.H. Laurindo, J.M.F. de Paiva Júnior, A. Lohrengel, and F.L. Amorim, Materials Used for Sinking EDM Electrodes: A Review, *J. Brazilian Soc. Mech. Sci. Eng.*, 2019, **41**(1), p 1–25. <https://doi.org/10.1007/s40430-018-1520-y>
6. W. Lu, M. Zu, J.-H. Byun, B.-S. Kim, and T.-W. Chou, State of the Art of Carbon Nanotube Fibers: Opportunities and Challenges, *Adv. Mater.*, 2012, **24**(14), p 1805–1833. <https://doi.org/10.1002/adma.201104672>
7. A. Lekawa-Raus, J. Patmore, L. Kurzepa, J. Bulmer, and K. Koziol, Electrical Properties of Carbon Nanotube Based Fibers and Their Future Use in Electrical Wiring, *Adv. Funct. Mater.*, 2014, **24**(24), p 3661–3682. <https://doi.org/10.1002/adfm.201303716>
8. P.L. McEuen and J.-Y. Park, Electron Transport in Single-Walled Carbon Nanotubes, *MRS Bull.*, 2004, **29**(4), p 272–275. <https://doi.org/10.1557/mrs2004.79>
9. O. Breuer and U. Sundararaj, Big Returns from Small Fibers: A Review of Polymer/Carbon Nanotube Composites, *Polym. Compos.*, 2004, **25**(6), p 630–645. <https://doi.org/10.1002/pc.20058>
10. M. Fujii, X. Zhang, H. Xie, H. Ago, K. Takahashi, T. Ikuta, H. Abe, and T. Shimizu, Measuring the Thermal Conductivity of a Single Carbon Nanotube, *Phys. Rev. Lett.*, 2005, **95**(6), p 065502. <https://doi.org/10.1103/PhysRevLett.95.065502>
11. D.J. Yang, Q. Zhang, G. Chen, S.F. Yoon, J. Ahn, S.G. Wang, Q. Zhou, Q. Wang, and J.Q. Li, Thermal Conductivity of Multiwalled Carbon Nanotubes, *Phys. Rev. B*, 2002, **66**(16), p 165440. <https://doi.org/10.1103/PhysRevB.66.165440>
12. E. Pop, D. Mann, Q. Wang, K. Goodson, and H. Dai, Thermal Conductance of an Individual Single-Wall Carbon Nanotube above Room Temperature, *Nano Lett.*, 2006, **6**(1), p 96–100. <https://doi.org/10.1021/nl052145f>
13. A.A. Khan, M.H.F. Al Hazza, E.Y.T. Adesta, and N.F.B. Mohd, “Modeling the Effect of CNT Concentration in Dielectric Fluid on EDM Performance Using Neural Network,” *2015 4th International Conference on Advanced Computer Science Applications and Technologies (ACSAT)*, (Kuala Lumpur, Malaysia), IEEE, 2015, p 266–270. <https://doi.org/10.1109/ACSAT.2015.24>
14. S. Mohal and H. Kumar, Study on the Multiwalled Carbon Nano Tube Mixed EDM of Al-SiC p Metal Matrix Composite, *Mater. Today: Proceed.*, 2017, **4**(2), p 3987–3993. <https://doi.org/10.1016/j.matpr.2017.02.299>
15. M. Danish, M. Al-Amin, S. Rubaiee, A.M. Abdul-Rani, F.T. Zohura, A. Ahmed, R. Ahmed, and M.B. Yildirim, Enhanced Machining Features and Multi-Objective Optimization of CNT Mixed-EDM Process for Processing 316L Steel, *Int. J. Adv. Manuf. Technol.*, 2022, **120**(9–10), p 6125–6141. <https://doi.org/10.1007/s00170-022-09157-5>
16. C. Mai, H. Hocheng, and S. Huang, Advantages of Carbon Nanotubes in Electrical Discharge Machining, *Int. J. Adv. Manuf. Technol.*, 2012, **59**(1–4), p 111–117
17. T. Suzuki, M. Kato, H. Saito, and H. Iizuka, Effect of Carbon Nanotube (CNT) Size on Wear Properties of Cu-Based CNT Composite Electrodes in Electrical Discharge Machining, *J. Solid Mech. Mater. Eng.*, 2011, **5**(7), p 348–359. <https://doi.org/10.1299/jmmp.5.348>
18. J. Choi, Y. Jung, S.J. Yang, J.Y. Oh, J. Oh, K. Jo, J.G. Son, S.E. Moon, C.R. Park, and H. Kim, Flexible and Robust Thermoelectric Generators Based on All-Carbon Nanotube Yarn without Metal Electrodes, *ACS Nano*, 2017, **11**(8), p 7608–7614. <https://doi.org/10.1021/acsnano.7b01771>
19. T. Watanabe, A. Itoh, T. Watanabe, T. Kizaki, M. Inaguma, A. Hosoi and H. Kawada, Post-Synthesis Treatment Improves the Electrical Properties of Dry-Spun Carbon Nanotube Yarns, *Carbon*, 2021, **185**, p 314–323. <https://doi.org/10.1016/j.carbon.2021.09.022>
20. D.E. Tsentelovich, R.J. Headrick, F. Mirri, J. Hao, N. Behabtu, C.C. Young, and M. Pasquali, Influence of Carbon Nanotube Characteristics on Macroscopic Fiber Properties, *ACS Appl. Mater. Interfaces*, 2017, **9**(41), p 36189–36198. <https://doi.org/10.1021/acsnano.7b10968>
21. P. Chaudhury and S. Samantaray, Role of Carbon Nano Tubes in Surface Modification on Electrical Discharge Machining -A Review, *Mater. Today Proc.*, 2017, **4**(2), p 4079–4088. <https://doi.org/10.1016/j.matpr.2017.02.311>
22. S. Kalpakjian, S.R. Schmid, and H. Musa, “Manufacturing Engineering and Technology,” Holly Stark and C. Romeo, Ed., 6th edn., (Prentice Hall, 2009)
23. M.P. Groover, *Fundamentals of Modern Manufacturing: Materials, Processes, and Systems*, J. Brady, Ed., 7th edn Wiley, 2019, https://books.google.com.tr/books?hl=tr&lr=&id=mB7zDwAAQBAJ&oi=fnd&pg=PA1&dq=Fundamentals+of+Modern+Manufacturing+_+Material+s,+Processes,+and+Systems&ots=H1cFk78oCX&sig=T9Rb2mOJ840yDFYId311EFB9F9U&redir_esc=y#v=onepage&q=Fundamentals of Modern Manufacturing
24. M. Miao, Yarn Spun from Carbon Nanotube Forests: Production, Structure, Properties and Applications, *Particuology*, Chinese Society of, *Particuology*, 2013, **11**(4), p 378–393. <https://doi.org/10.1016/j.partic.2012.06.017>
25. Y. Dini, D. Rouchon, J. Faure-Vincent, and J. Dijon, Large Improvement of Electrical Conductivity by Varying Chemical Doping and

- Annealing Treatment, *Carbon N. Y.*, 2020, **156**, p 38–48. <https://doi.org/10.1016/j.carbon.2019.09.022>
26. M. Kunieda, M. Yoshida, and N. Taniguchi, Electrical Discharge Machining in Gas, *CIRP Ann.*, 1997, **46**(1), p 143–146. [https://doi.org/10.1016/S0007-8506\(07\)60794-X](https://doi.org/10.1016/S0007-8506(07)60794-X)
 27. N.P. Hiremath, “Structure And Properties Of Cnt Yarns And Cnt / Cnf Reinforced Pan- Based Carbon Fibers,” University of Tennessee, 2016, http://trace.tennessee.edu/cgi/viewcontent.cgi?article=5412&context=utk_graddiss
 28. M. Miao, Electrical Conductivity of Pure Carbon Nanotube Yarns, *Carbon N. Y.*, 2011, **49**(12), p 3755–3761. <https://doi.org/10.1016/j.carbon.2011.05.008>
 29. M. Miao, J. McDonnell, L. Vuckovic, and S.C. Hawkins, Poisson’s Ratio and Porosity of Carbon Nanotube Dry-Spun Yarns, *Carbon N. Y.*, 2010, **48**(10), p 2802–2811. <https://doi.org/10.1016/j.carbon.2010.04.009>
 30. V. Sabelkin, H.E. Misak, S. Mall, R. Asmatulu, and P.E. Kladitis, Tensile Loading Behavior of Carbon Nanotube Wires, *Carbon N. Y.*, 2012, **50**(7), p 2530–2538. <https://doi.org/10.1016/j.carbon.2012.01.077>
 31. B. Bhattacharyya and B. Doloi, “Modern Machining Technology: Advanced, Hybrid, Micro Machining and Super Finishing Technology,” B. Guerin, Ed. (Academic Press, 2019, https://books.google.com.tr/books?hl=tr&lr=&id=eEOwDwAAQBAJ&oi=fnd&pg=PP1&dq=modern+Machining&ots=sbFqPW1S-Y&sig=_Q-rQgRM89fzCd8Zt7Bki0jp60c&redir_esc=y#v=onepage&q&f=false. Accessed 7 December 2021)
 32. R. Ji, Y. Liu, R. Diao, X. Chenchen, X. Li, B. Cai, and Y. Zhang, Influence of Electrical Resistivity and Machining Parameters on Electrical Discharge Machining Performance of Engineering Ceramics, *PLoS ONE*, 2014, **9**(11), p e110775. <https://doi.org/10.1371/journal.pone.0110775>
 33. M. Miao, Carbon Nanotube Yarns for Electronic Textiles, *Electron. Text.*, 2015 <https://doi.org/10.1016/B978-0-08-100201-8.00004-7>
 34. Y. Zhao, M. Kunieda, and K. Abe, Study of EDM Cutting of Single Crystal Silicon Carbide, *Precis. Eng.*, 2014, **38**(1), p 92–99. <https://doi.org/10.1016/j.precisioneng.2013.07.008>
 35. Y. Zhang, Y. Liu, R. Ji, and B. Cai, Study of the Recast Layer of a Surface Machined by Sinking Electrical Discharge Machining Using Water-in-Oil Emulsion as Dielectric, *Appl. Surf. Sci.*, 2011, **257**(14), p 5989–5997. <https://doi.org/10.1016/j.apsusc.2011.01.083>
 36. Z. Yu, T. Jun, and K. Masanori, Dry Electrical Discharge Machining of Cemented Carbide, *J. Mater. Process. Technol.*, 2004, **149**(1–3), p 353–357. <https://doi.org/10.1016/j.jmatprotec.2003.10.044>
 37. M. Kunieda, Y. Miyoshi, T. Takaya, N. Nakajima, Y. ZhanBo, and M. Yoshida, High Speed 3D Milling by Dry EDM, *CIRP Ann.*, 2003, **52**(1), p 147–150. [https://doi.org/10.1016/S0007-8506\(07\)60552-6](https://doi.org/10.1016/S0007-8506(07)60552-6)
 38. P.M. Ajayan, and S. Iijima, Capillarity-Induced Filling of Carbon Nanotubes, *Nature*, 1993, **361**(6410), p 333–334. <https://doi.org/10.1038/361333a0>
 39. P.M. Ajayan, T.W. Ebbesen, T. Ichihashi, S. Iijima, K. Tanigaki, and H. Hiura, Opening Carbon Nanotubes with Oxygen and Implications for Filling, *Nature*, 1993, **362**(6420), p 522–525. <https://doi.org/10.1038/362522a0>
 40. T.J. Kang, T. Kim, S.M. Seo, Y.J. Park, and Y.H. Kim, Thickness-Dependent Thermal Resistance of a Transparent Glass Heater with a Single-Walled Carbon Nanotube Coating, *Carbon N. Y.*, 2011, **49**(4), p 1087–1093. <https://doi.org/10.1016/j.carbon.2010.11.012>
 41. N. Yao, V. Lordi, S.X.C. Ma, E. Dujardin, A. Krishnan, M.M.J. Treacy, and T.W. Ebbesen, Structure and Oxidation Patterns of Carbon Nanotubes, *J. Mater. Res.*, 1998, **13**(9), p 2432–2437. <https://doi.org/10.1557/JMR.1998.0338>
 42. H. Rho, M. Park, M. Park, J. Park, J. Han, A. Lee, S. Bae, T.-W. Kim, J.-S. Ha, S.M. Kim, D.S. Lee, and S.H. Lee, Metal Nanofibrils Embedded in Long Free-Standing Carbon Nanotube Fibers with a High Critical Current Density, *NPG Asia Mater.*, 2018, **10**(4), p 146–155. <https://doi.org/10.1038/s41427-018-0028-3>
 43. J. S. Bulmer, A. Kaniyoor, and J. A. Elliott, A Meta-Analysis of Conductive and Strong Carbon Nanotube Materials, *Adv. Mater.*, 2021, **33**(36), p 2008432. <https://doi.org/10.1002/adma.202008432>
 44. X. Wang, N. Behabtu, C.C. Young, D.E. Tsentelovich, M. Pasquali, and J. Kono, High-Ampacity Power Cables of Tightly-Packed and Aligned Carbon Nanotubes, *Adv. Funct. Mater.*, 2014, **24**(21), p 3241–3249
 45. D. Sharma and S. S. Hiremath, Review on Tools and Tool Wear in EDM, *Mach. Sci. Technol.*, 2021, **25**(5), p 802–873. <https://doi.org/10.1080/10910344.2021.1971711>
 46. C.C. Kao, J. Tao, and A.J. Shih, Near Dry Electrical Discharge Machining, *Int. J. Mach. Tools Manuf.*, 2007, **47**(15), p 2273–2281. <https://doi.org/10.1016/j.ijmachtools.2007.06.001>
 47. A. Jorio, G. Dresselhaus, and M.S. Dresselhaus Eds., *Carbon Nanotubes: Advanced Topics in the Synthesis, Structure, Properties and Applications*, Springer Berlin Heidelberg, Berlin, Heidelberg, 2008
 48. Michael J. O’Connell, Ed., “Carbon Nanotubes: Properties and Applications,” (CRC Press Taylor & Francis Group, 2006)
 49. N. Mohri, M. Suzuki, M. Furuya, N. Saito, and A. Kobayashi, Electrode Wear Process in Electrical Discharge Machinings, *CIRP Ann.*, 1995, **44**(1), p 165–168 [https://doi.org/10.1016/S0007-8506\(07\)62298-7](https://doi.org/10.1016/S0007-8506(07)62298-7)
 50. S.L. Chen, B.H. Yan, and F.Y. Huang, Influence of Kerosene and Distilled Water as Dielectrics on the Electric Discharge Machining Characteristics of Ti–6Al–4V, *Journal of Materials Processing Technology*, 1999, **87**(1–3), p 107–111. [https://doi.org/10.1016/S0924-0136\(98\)00340-9](https://doi.org/10.1016/S0924-0136(98)00340-9)
 51. Y. Jung, YSh. Cho, J.W. Lee, Oh. Jun Young, and C.R. Park, How Can We Make Carbon Nanotube Yarn Stronger?, *Comp. Sci. Technol.*, 2018, **166**, p 95–108. <https://doi.org/10.1016/j.compscitech.2018.02.010>
 52. A.M. Beese, X. Wei, S. Sarkar, R. Ramachandramoorthy, M.R. Roenbeck, A. Moravsky, M. Ford, F. Yavari, D.T. Keane, R.O. Loutfy, S.T. Nguyen, and H.D. Espinosa, Key Factors Limiting Carbon Nanotube Yarn Strength: Exploring Processing-Structure-Property Relationships, *ACS Nano*, 2014, **8**(11), p 11454–11466. <https://doi.org/10.1021/nn5045504>
 53. J. Di, S. Fang, F.A. Moura, D.S. Galvão, J. Bykova, A. Aliev, M.J. de Andrade, X. Lepró, N. Li, C. Haines, R. Ovalle-Robles, D. Qian, and R.H. Baughman, Strong, Twist-Stable Carbon Nanotube Yarns and Muscles by Tension Annealing at Extreme Temperatures, *Adv. Mater.*, 2016, **28**, p 6598–6605
 54. M. Dahmardeh, A. Nojeh, and K. Takahata, Possible Mechanism in Dry Micro-Electro-Discharge Machining of Carbon-Nanotube Forests: A Study of the Effect of Oxygen, *J. Appl. Phys.*, 2011, **109**(9), p 1–4
 55. F. Deng, W. Lu, H. Zhao, Y. Zhu, B.-S. Kim, and T.-W. Chou, The Properties of Dry-Spun Carbon Nanotube Fibers and Their Interfacial Shear Strength in an Epoxy Composite, *Carbon N. Y.*, 2011, **49**(5), p 1752–1757. <https://doi.org/10.1016/j.carbon.2010.12.061>
 56. D. Li, Q.-S. Yang, X. Liu, and J.-J. Shang, Experimental Investigation on Tensile Properties of Carbon Nanotube Wires, *Mech. Mater.*, 2017, **105**, p 42–48. <https://doi.org/10.1016/j.mechmat.2016.11.010>
 57. J. Tao, A.J. Shih, and J. Ni, Experimental Study of the Dry and Near-Dry Electrical Discharge Milling Processes, *J. Manuf. Sci. Eng.*, 2008, **10**(1115/1), p 2784276

Publisher’s Note Springer Nature remains neutral with regard to jurisdictional claims in published maps and institutional affiliations.

Springer Nature or its licensor (e.g. a society or other partner) holds exclusive rights to this article under a publishing agreement with the author(s) or other rightsholder(s); author self-archiving of the accepted manuscript version of this article is solely governed by the terms of such publishing agreement and applicable law.